



Performance of Self-Compacting mortars modified with Nanoparticles: A systematic review and modeling



Rabar H. Faraj^{a,b}, Hemn Unis Ahmed^{a,*}, Serwan Rafiq^a, Nadhim Hamah Sor^c, Dalya F. Ibrahim^b, Shaker M.A. Qaidi^d

^a Civil Engineering Department, College of Engineering, University of Sulaimani, Sulaimani, Kurdistan Region, Iraq

^b Civil Engineering Department, University of Halabja, Halabja, Kurdistan Region, Iraq

^c Civil Engineering Department, University of Garmian, Kalar, Kurdistan Region, Iraq

^d Department of Civil Engineering, College of Engineering, University of Duhok, Duhok, Kurdistan Region, Iraq

ARTICLE INFO

Keywords:

Self-compacting mortar
Nanoparticles
Mechanical properties
Fresh properties
Durability
Modeling

ABSTRACT

During the transition of one material from macro- to nano-range size, considerable changes occur in the electron conductivity, optical absorption, mechanical properties, chemical reacting activity, and surface morphology. These changes can be advantageous in the production of new mixture composites. Due to the need for developing improved infrastructure, new and high-performance materials should also be developed. In this regard, to improve the performance of concrete mixtures, several methods have been investigated, including using nanoparticles (NPs) to enhance various characteristics of the concrete composite like improving fresh and mechanical properties of self-compacting concrete (SCC) as well as improving permeability and absorption capacity of the composite by providing extremely fine particles to fill micro-pores and voids.

In this paper, a state-of-the-art review was carried out on the influence of various NPs inclusion on the fresh, mechanical, and durability properties of self-compacting mortars (SCM). So that current and most recent studies previously published were investigated to highlight the influences of different NPs on the slump flow diameter, V-funnel flow time, compression and flexural strengths, water absorption, chloride penetration, and electrical resistivity. Moreover, the main section of this study was devoted to proposing different models, including nonlinear model (NLR), multi-logistic model (MLR), and artificial neural network (ANN), to predict the compressive strength (CS) of SCMs modified with NPs. Based on the analyzed data, it was illustrated that the addition of NPs into SCMs significantly enhances the fresh, mechanical, and durability performance of SCMs. Moreover, the microstructure of SCMs was considerably improved due to the higher specific surface area of NPs and their reaction with undesirable C–H which present in the cement paste matrix to produce additional C-S-H gel.

1. Introduction

In the concrete industry, the invention of self-compacting concrete (SCC) could be considered an excellent achievement for humanity due to the variety of benefits. However, one of the drawbacks of this type of concrete is that it consumes a larger volume of cement paste fractions as compared to conventional concrete composites, which lead to a rise in the cost of the materials and affect other vital characteristics of the concrete composite (Faraj et al. 2019; Faraj et al. 2020, Faraj et al. 2021a). One of the essential properties of the SCC is flow and spread inside the concrete formwork under its weight without using any vibration and compaction, as well as no bleeding and segregation

appearing after removal of the concrete formworks. SCC is a new generation of conventional concrete, an ideal candidate for concrete structural elements with a high percent of reinforcements.

On the other hand, due to the benefit that SCM offers compared to traditional mortar, the usage of SCM is one of the most active research areas in the branch of civil engineering, especially in construction materials (Mohseni and Tsavdaridis, 2016a). SCM can be considered an ideal material for repairing and rehabilitation of reinforced concrete (RC) elements (Courard et al. 2002).

Nanomaterials are a new material in the civil engineering field, and nanotechnology has been used in many applications and products (Ahmed et al., 2022a). The application of nanomaterials inside con-

* Corresponding author..

E-mail address: hemn.ahmed@univsul.edu.iq (H.U. Ahmed).

ventional cement-based mortar and concrete has been widely investigated by researchers (Lazaro et al. 2016; Shahbazpanahi et al. 2021a). Generally, nanotechnology is the monitoring capability and restructure of the matter at the atomic and molecular levels in the area of 1 to 100 nm, and contribution to the distinguished characteristics and phenomena at that size as equivalent to those correlating with single atoms and molecules or bulk behavior (Zhu et al. 2004; Sharif, 2021; Faraj et al. 2022).

In the past, various researches were carried out to study different characteristics of SCMs containing different types of NPs (Madandoust et al. 2015; Mohseni et al. 2015; Kadhim et al. 2020; Khotbehsara et al. 2015; Miyandehi et al. 2014). Among the various NPs used in the previous investigations, nano SiO_2 (NS) is the most popular. Other types of NPs used in the literature include Nano Al_2O_3 (NA) (Mohseni et al. 2015; Mohseni and Tsavdaridis, 2016a; Miyandehi et al. 2014), Nano TiO_2 (NT) (Mohseni et al. 2015; Mohseni et al., 2016b; Rao et al. 2015), Nano Fe_2O_3 (NF) (Madandoust et al. 2015), Nano CuO (NC) (Khotbehsara et al. 2015; Mohseni et al. 2015), Nano cement kiln dust (NCKD) (Kadhim et al. 2020), Nano ZnO_2 (NZn) and Nano Cr_2O_3 (NCr) (Yang et al. 2015).

The main reason for adding NPs into all types of concrete composites, including SCM and SCC is to enhance the microstructural characteristics of the concrete composite. As a result, it would improve all other composite properties, namely mechanical and physical properties and durability properties of the concrete composites (Balapour et al. 2018). The main product in the hydration process between cement and water is the calcium silicate hydrate (C-S-H) gel and calcium hydroxide (C-H) crystals (Shahbazpanahi and Faraj, 2020; Shahbazpanahi et al. 2021b). However, C-H crystals are an unwanted product in the concrete composite matrix because they lead to some drawbacks in the nearer future in the cement matrix and consequently adversely affect the concrete performance. To tackle these problems of C-H crystals in the concrete composite matrix, some researchers add nano-silica to the concrete composite to change the undesired C-H crystals to the C-S-H gels in the chemical reaction process, namely pozzolanic reaction. As a result of this pozzolanic reaction, extra C-S-H gel is generated, and the presence of C-H crystals is reduced inside the concrete composite matrix; and finally, the performance and microstructure of the concrete composite are improved (Thomas et al. 2017).

This review study aims to investigate the influence of various NPs inclusion on the fresh, strength, and durability performance of SCMs. In the literature, no review paper was found to summarize the effect of NPs on the performance of SCMs. Therefore, in this study, the previous researches were investigated to highlight the effects of NPs on the most critical fresh, mechanical, and durability properties of SCMs such as slump flow diameter, V-funnel flow time, compression strength, flexural strength, water absorption capacity, chloride penetration, and electrical resistivity. Moreover, an empirical model among strength properties is also developed. Moreover, a significant part of this study is devoted to proposing systematic multiscale models to forecast the CS of SCMs containing NPs. Various mixture proportions and curing times were used as input parameters to develop reliable models to predict the CS. Based on the best of the author's knowledge, this is the first review paper on this topic, including a systematic review, analysis, and modeling. This study encourages the construction industry to take advantage of nanotechnology to produce high-performance cement-based materials that can be used to develop improved infrastructure.

2. Properties of NPs and SCM mixes used in the literature

In this section, different types and properties of NPs used in the literature to improve the performance of SCMs are reported. Moreover, additional information regarding the mixed proportions of SCMs made

with various types of NPs are present in Table 1. The amount of NPs used in the mixed proportions of SCMs is between 0% and 5% replacements with cement by weight. Higher amounts of NPs could diminish their advantage due to their agglomeration inside the matrix, which aggravates the fresh flow behavior of SCMs. The diameter of NPs varied between 15 and 62.3 nm, with the surface–volume ratio ranging from 50 to 230 m^2/g . The majority of the NPs shapes used in the previous studies are spherical as illustrated in Fig. 1, which explains the nano CuO (NCu) particles using transmission electron micrographs (TEM).

3. Properties of SCM containing different NPs

The main focus of this study is to review the fresh, strength, and durability performance of SCMs made with different types of NPs. Therefore, the following section reports the results obtained from previous studies and the proper discussion for each property will also present.

3.1. Rheological and fresh properties

As mentioned previously, SCM is a mixture with a high flowability compared to conventional mortar. Therefore, assessing this composite in the fresh state is quite critical. The fresh and rheological behavior of SCC and SCM can be assessed through the tests outlined in (EFNARC, 2002; ASTM C-1437–2003). The most common tests to assess the fresh behavior of SCMs are mini-slump and V-funnel.

For the mini-slump test, the apparatus is in the cone shape, having the dimensions (height = 60 mm, diameter at the base = 100 mm and top diameter = 70 mm) as shown in Fig. 2a. The cone is filled with SCM, then gently lifted upwards. As a result, the mortar spreads over the steel base plate and the diameter of the spread mortar is recorded in two opposite directions and the average is calculated as the diameter for the test.

For the mini V-funnel test, which is generally used to assess the filling ability and determine a proper water/ binder ratio for the SCM mixtures, a mini funnel is poured with SCM mixture; the bottom gate of the funnel is then opened and the time is start recording. When the light first appeared by looking down into the funnel, the time is stopped, and the flow time in seconds is recorded. Fig. 2b illustrates the mini V-funnel instrument and conducting the test.

3.1.1. Slump flow diameter

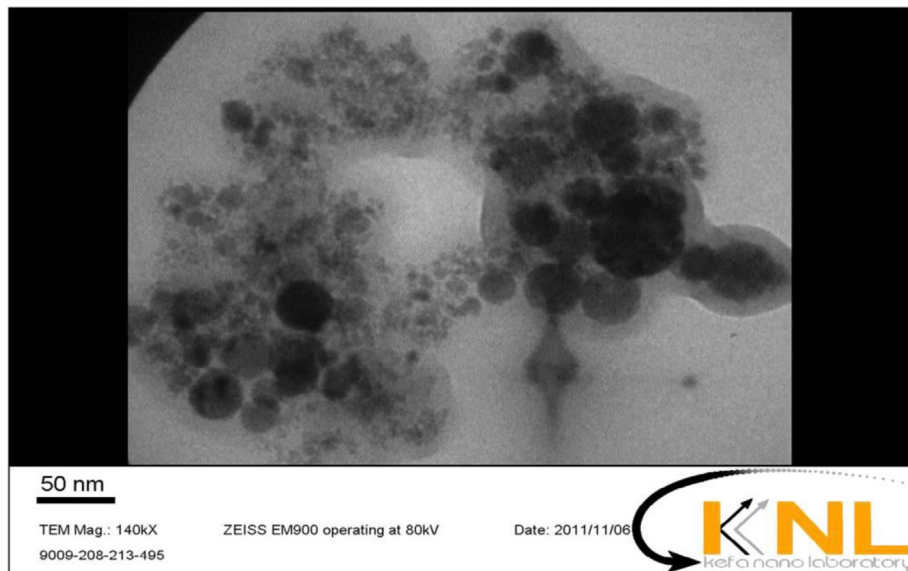
The experimental outcomes extracted from past investigations for the SCMs containing different replacement percentages of NPs are presented in Fig. 3. The higher slump values mean the higher workability for the SCM mixtures. The slump flow diameters of SCMs containing different types of NPs reported in the literature varied between 240 mm and 260 mm, except the mixture contained NCKD, which reported higher values (Kadhim et al. 2020). As shown in Fig. 3, except for the NCKD, all other NPs had a similar influence on the slump values of SCMs. Slump flow diameter was slightly elevated with changing the NPs percentage from 0% to 5%. Mohseni and Tsavdaridis (2016a) investigated the impact of NA particles on the fresh performance of SCMs. Three different proportions of NA particles (1, 3, and 5%) of the binder content were incorporated. They observed that the slump flow diameter increased slightly with increasing the NA particles content. The control mixture had a flow diameter of 245 mm, then it was boosted to 250 mm when 5% of NA particles were utilized. Similar observations for other types of NPs were also presented by other researchers (Madandoust et al. 2015; Nasr et al. 2019; Mohseni et al. 2015). The main reason behind increasing the slump diameter value due to the addition of NPs is that a higher amount of superplasticizer is required for the mixtures made with NPs. Because the NPs had a very high surface area compared to cement particles, it is expected

Table 1

Properties of NPs and SCM mixtures reported in the literature.

Refs.	Composite types	Cement replacement with NPs: wt%	Binder content	w/b ratio	Curing time (days)	Properties of NPs
Madandoust et al. 2015	SCM	0, 1, 2, 3, 4, 5	700	0.4	3, 7, 28, 90 days	D (nm) = 15 SVR (m^2/g) = 200 Purity (%) > 99 D (nm) = 60 SVR (m^2/g) = 60 Purity (%) > 98 D (nm) = 15 SVR (m^2/g) = 200 Purity (%) > 99
Mohseni et al. 2015	SCM	0, 1, 3, 5	700	0.4	3, 7, 28, 90 days	D (nm) = 15 ± 3 SVR (m^2/g) = 200 Purity (%) > 99
Mohseni and Tsavdaridis, 2016a	SCM	0, 1, 3, 5	700	0.4	3, 7, 28, 90 days	D (nm) = 15 ± 3 SVR (m^2/g) = 200 Purity (%) > 99
Mohseni et al., 2016b	SCM	0, 1, 3, 5	700	0.4	3, 7, 28, 90 days	D (nm) = 15 ± 3 SVR (m^2/g) = 200 Purity (%) > 99
Kadhim et al. 2020	SCM	0, 1, 2, 3, 4, 5	600	0.35	7, 28, 90 days	D (nm) = 62.3 Purity (%) > 99.9
Khotbehsara et al. 2015	SCM	0, 1, 2, 3, 4	700	0.4	7, 28, 90 days	D (nm) = 15 ± 3 SVR (m^2/g) = 165 ± 17 Purity (%) > 99.9
Khotbehsara et al. 2018	SCM	0, 1, 2, 3, 4, 5	700	0.4	3, 7, 28, 90 days	D (nm) = 20 ± 3 SVR (m^2/g) = 200 Purity (%) > 99
Miyandehi et al. 2014	SCM	0, 1, 3, 5	700	0.4	3, 7, 28, 90 days	D (nm) = 15 SVR (m^2/g) = 200 Purity (%) > 99.8
Nasr et al. 2019	SCM	0, 1, 2, 3, 4	550	0.5	3, 7, 28, 90 days	D (nm) = 20–30 SVR (m^2/g) = 230 Purity (%) > 99
Rao et al. 2015	SCM	0, 0.5, 0.75, 1 0, 0.75, 1.5, 3	700	0.43	7, 28, 90 days	D (nm) = 20 SVR (m^2/g) = 260 D (nm) = 20 SVR (m^2/g) = 50
Yang et al. 2015	SCM	0, 1, 2, 3, 4, 5	700	0.4	3, 7, 28, 90 days	D (nm) = 15 SVR (m^2/g) = 200 ± 30

SVR = Surface to volume ratio, D = diameter.

**Fig. 1.** NCu particles observed using TEM (Khotbehsara et al. 2015).

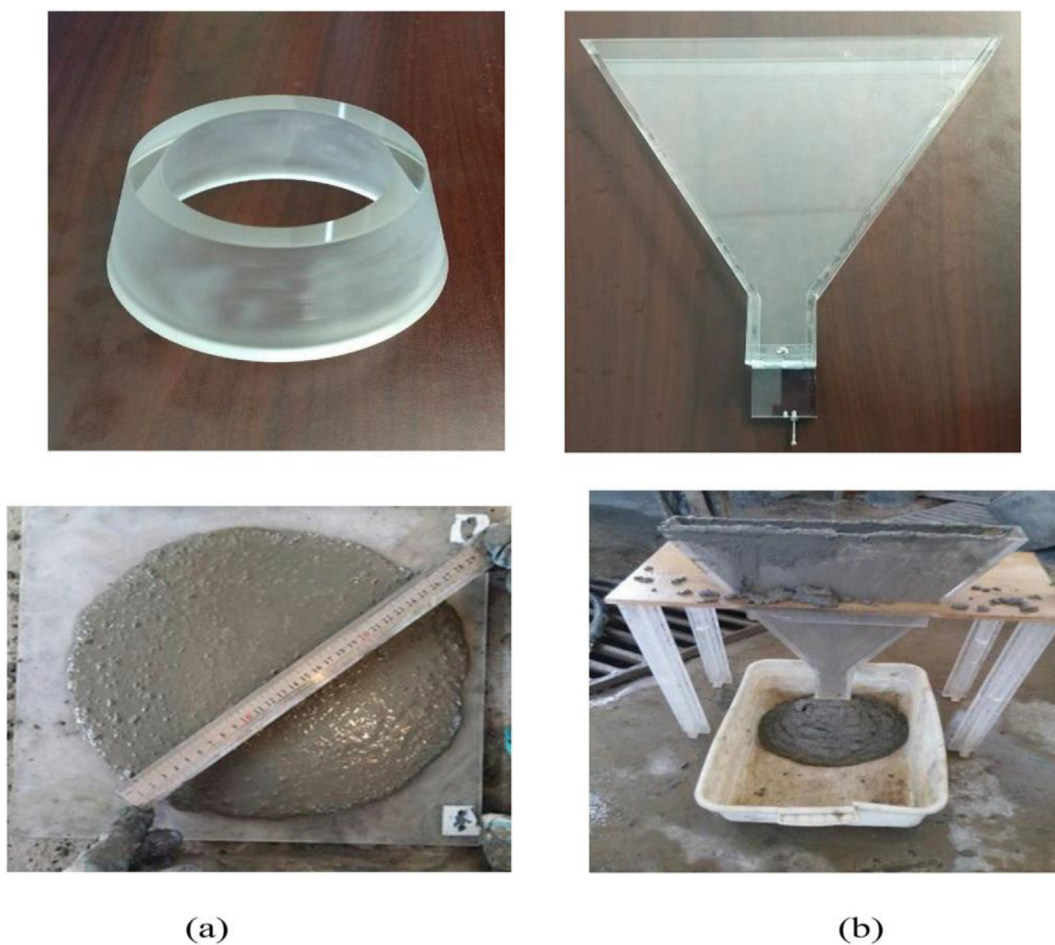


Fig. 2. Rheological tests for measuring fresh properties of SCM: (a) mini slump, (b) v-funnel ([Jalal et al. 2019](#)).

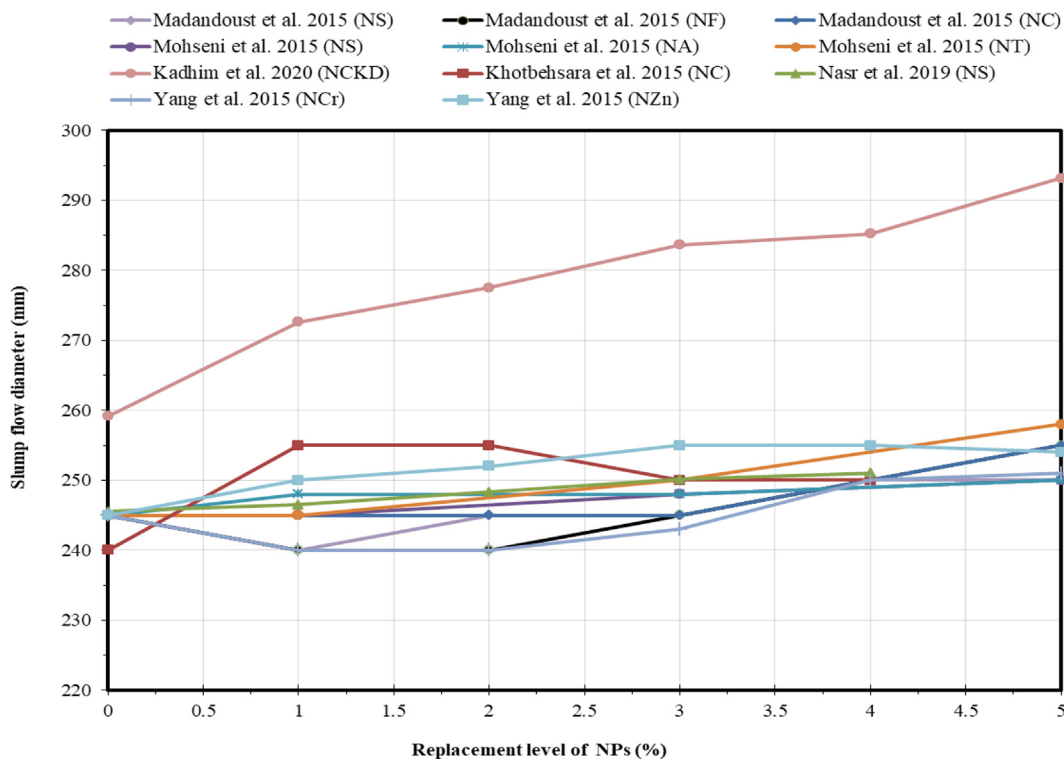


Fig. 3. Slump flow values versus replacement amount of NPs reported in previous studies.

to reduce the slump diameter, and a higher amount of water is required to hydrate the particles. However, adding a higher dosage of superplasticizer compensated the effect of surface area and made the mixtures higher slump values (Rao et al. 2015).

3.1.2. V-funnel Flow time

Fig. 4 reports the experimental results for the V-funnel flow time of SCMs containing different dosages of NPs obtained from past studies. Opposite to slump flow diameter, higher times of V-funnel flow test represents less workability because the mixture needs more time to empty the funnel, which also means lower filling ability. As seen from the Figure, different results were reported in the literature. Some researchers reported that V-funnel flow time was decreased with increasing NPs content (Mohseni et al. 2015; Mohseni and Tsavdaridis, 2016a; Kadhim et al. 2020; Miyandehi et al. 2014). However, the opposite results were also presented by other scholars (Rao et al. 2015; Khotbehsara et al. 2018). Moreover, the fluctuated behavior was also recorded by some investigators (Khotbehsara et al. 2015; Madandoust et al. 2015). These different behaviors may be attributed to different studies having different mixture variables and the amount of NPs. For example, if the amount of superplasticizer was kept constant, the V-funnel flow time was elevated due to increasing the NPs content because the mixture's viscosity was increased and the mixture was more sticky, which requires higher time to empty the funnel (Rao et al. 2015). However, if the superplasticizer dosage was increased along with increasing the NPs content, the superplasticizer could compensate for the effects of NPs; consequently, the V-funnel flow time was decreased, and the workability of the mixture increased (Kadhim et al. 2020; Miyandehi et al. 2014).

3.2. Compressive and flexural strength

The compression strength (CS) results for the SCMs made with different NPs obtained from past studies are shown in Fig. 5. The results

demonstrated that the CS of SCMs was slightly improved with increasing the NPs content up to a particular percentage replacement, regardless of the NPs type. Generally, Increasing NPs content beyond 3% replacement by cement weight was no longer beneficial for improving the CS. This can be explained since, when the amount of NPs is high, the NPs cannot be dispersed well inside the matrix, and as a result, weak zones are formed due to NPs agglomeration and aggregation, causing the reduction of CS (Madandoust et al. 2015). The 28 days CS was in the range of 37 to 49 MPa, which is suitable for most structural applications. The main reason behind the enhancement of CS with the addition of NPs is that higher specific surface area of NPs and their reaction with undesirable C–H which present in the cement paste matrix to produce additional C–S–H, the microstructure of SCMs was considerably enhanced, and the number of pores was reduced; thus the compressive strength increased (Mohseni et al. 2015).

Fig. 6 shows the 28-day flexural strength results of SCMs containing various types and amounts of NPs. Research on the flexural strength of SCMs made with NPs is limited compared to compressive strength, and similar behavior for compressive strength was also reported for flexural strength. The addition of NPs slightly increased the flexural strength (Kadhim et al. 2020; Miyandehi et al. 2014). Miyandehi et al. 2014 found that the flexural strength was improved by about 13.8% when 3% of NA particles were added to the SCM mixture. They also reported that this improvement might be because NA particles could arrest cracks and interlocking influences between the slip planes; as a result, the flexural strength was enhanced.

To find an empirical relationship between the flexural and CS, the results obtained in the past studies are plotted in Fig. 7. As can be seen from the Figure, a strong polynomial relationship with the R^2 equal to 0.79 existed between the compressive and flexural strength. This empirical model can be helpful from the practical point of view for determining flexural strength from compressive strength since the flexural tests are not conducted commonly for SCMs containing NPs.

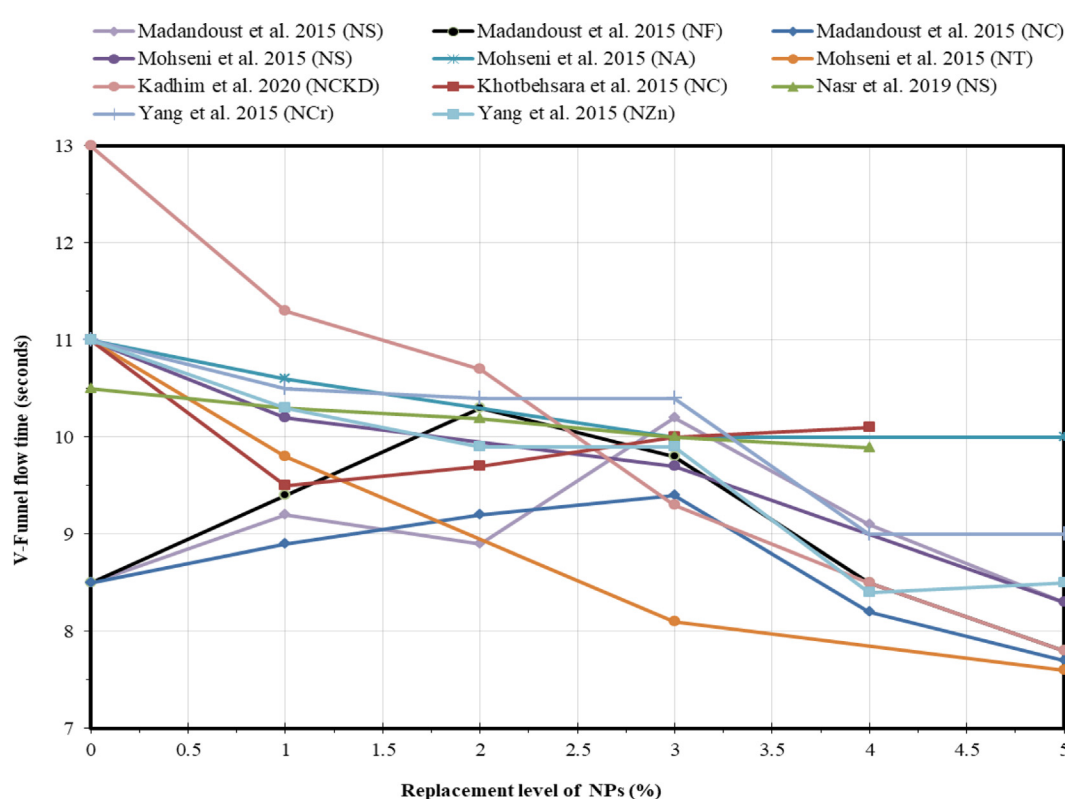


Fig. 4. V-funnel flow times versus replacement amount of NPs reported in previous studies.

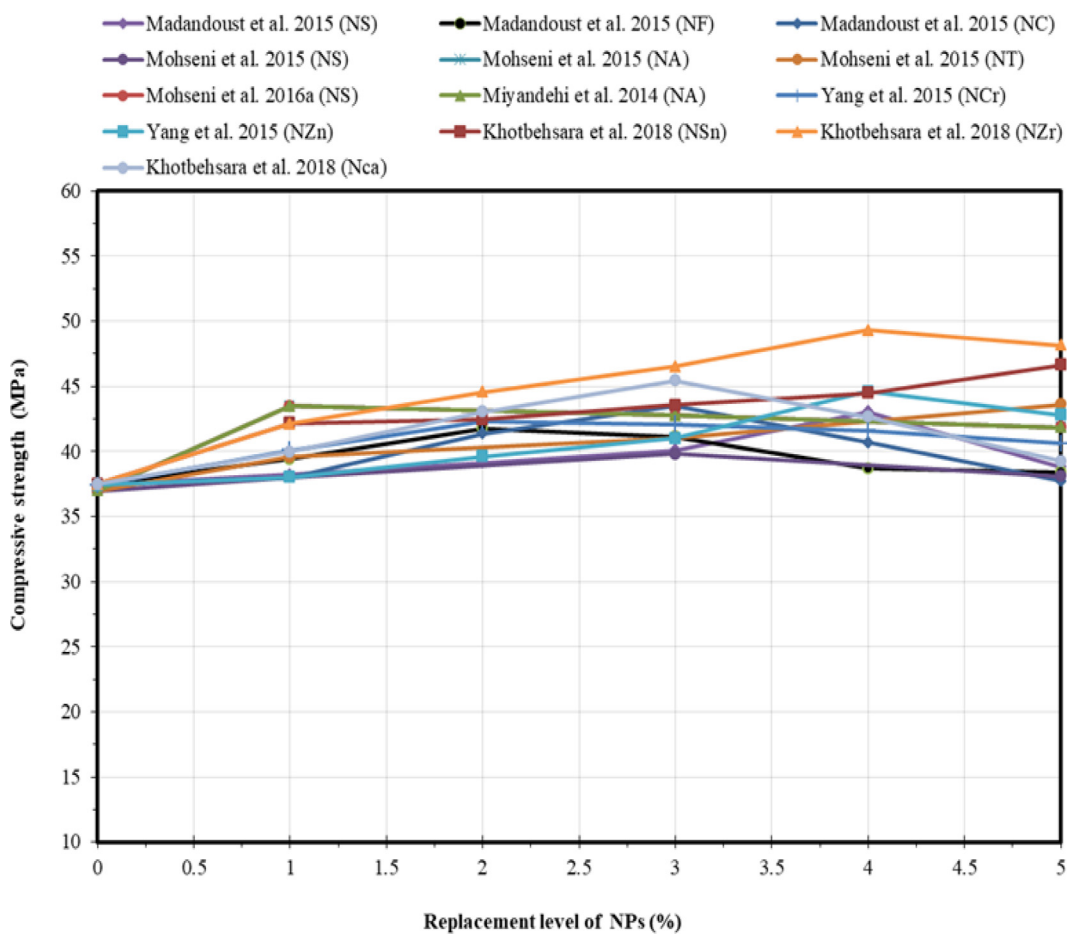


Fig. 5. Compressive strength versus replacement amount of NPs reported in previous studies at 28 days.

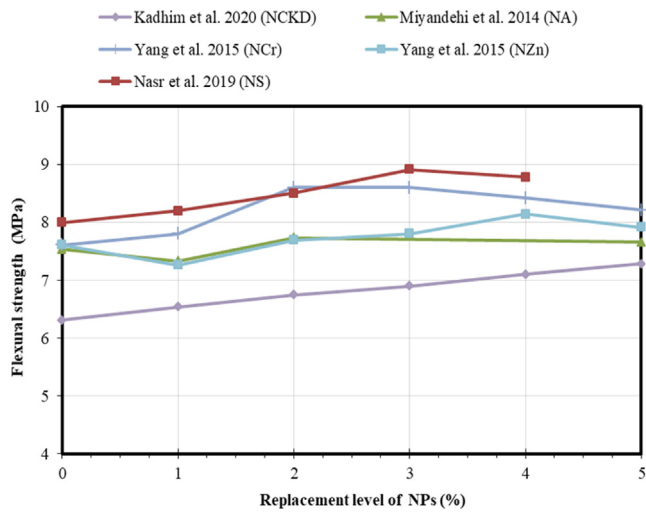


Fig. 6. Flexural strength versus replacement amount of NPs reported in previous studies at 28 days.

3.3. Durability performance

3.3.1. Water absorption

Generally, the water absorption (WA) test evaluated the performance against the penetration and retaining water. This test can be performed according to the procedures reported in (ASTM C642,

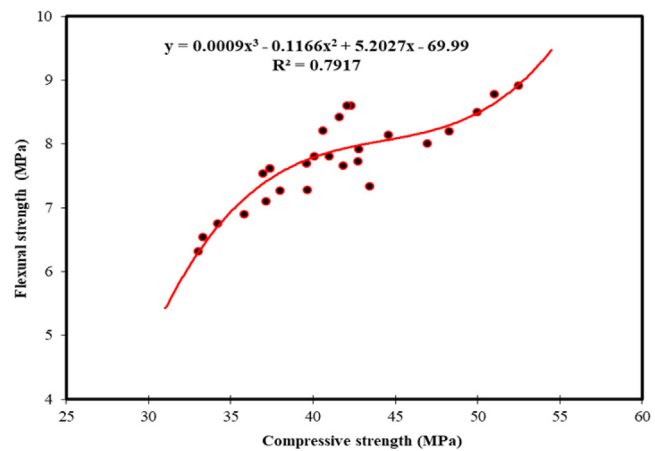


Fig. 7. Flexural strength versus compressive strength for SCMs containing NPs.

2013). The procedure required that the samples be cured for 28 days, then dried in an oven at a degree of 110 °C. Then the samples were required to be immersed in water at nearly 21 °C for 48 h. Finally, the saturated mass can be measured, and the WA can be determined.

The results of the previous studies regarding the water absorption of SCMs containing NPs are presented in Fig. 8. The previous results demonstrated that with the addition of NPs into SCM, the percentage of water absorption was reduced slightly. Madandoust et al. 2015

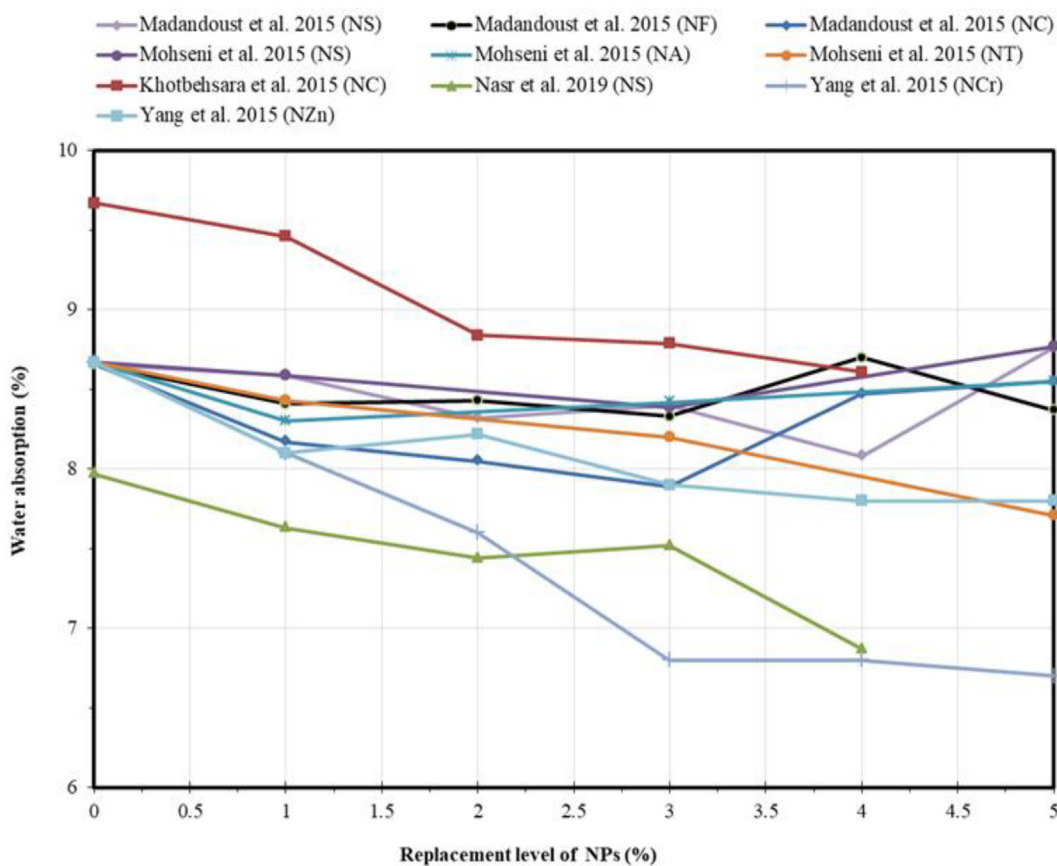


Fig. 8. Percentage of water absorption versus replacement amount of NPs reported in previous studies.

investigated the impact of NS, NF and NC on the durability performance of SCMs. They found that the inclusion of NPs reduced the WA of the samples, excluding the samples made with 5% NS and 4% NF. Compared to the reference sample, the highest percentage decrease of WA was 6% for the samples included 4% NS, 4% for the mixture containing 3% NF, and 9% for the mixture containing 3% NC. This behavior demonstrated that for different types of NPs an optimum percentage should be determined since further increase will not be beneficial regarding the improvement of WA. The explanation for this phenomenon is that, since the SVR was very high for all NP types, aggregation and agglomeration of the particles occurred at higher percentage contents, causing non-homogeneous dispersion of the NPs inside the SCM mixes (Madandoust et al. 2015).

Moreover, Mohseni et al. 2015 found that the inclusion of 5% NT resulted in the highest depletion of water absorption compared to the same percentage replacements of NS and NA. Similar findings for other types of NPs were also reported in different studies (Khotbehsara et al. 2015; Nasr et al. 2019; Yang et al. 2015). The reduction of water absorption due to the addition of NPs can be related to the fact that the NPs had a very small particles diameter compared to cement particles; thus, during hydration, they fill the small voids between cement particles, resulting in the denser matrix.

3.3.2. Electrical resistivity

One of the most important tests that can measure concrete's durability is the electrical resistivity test. The electrical resistivity test can measure and assess the sensitivity and resistance of SCMs to corrosion when a metal such as rebars is present inside the matrix. This test can be conducted following the guidelines of (ACI 222, 2001) on cubic samples with 50 mm dimensions, preferably after 90 days of curing. The apparatus used for the test consisted of an electrical resistance

device for measurements and two electrodes connected to opposite sides of the specimen. The electrical resistivity (ρ) is determined using the following formula:

$$\rho = \frac{RA}{L} \quad (1)$$

where R, A and L are the resistance (Ω), area of the specimen (cm^2), and length of the specimen (cm), respectively. Moreover, The electrical resistivity values and corrosion rate relationship is given in Table 2 to assess the durability performance of SCMs. As seen from the table, the higher electrical resistivity indicated a lower corrosion rate and better performance for the mixes.

The results of previous research regarding the influence of NPs on the electrical resistivity values of SCMs are presented in Fig. 9. The results can be used to indicate the corrosion probability level of the mixtures. The results demonstrated that mixtures containing 0% NPs (control mixtures) are located in the high corrosion rate level, while the addition of NPs shifted the corrosion rate level from high to low depending on the amount of NPs replacement. Different types of NPs had a dissimilar influence on electrical resistivity values, and the fluctuated behavior was observed for the majority of NP types. Mohseni

Table 2
Corrosion rate and electrical resistivity relationship (ACI 222, 2001).

Corrosion rate	Electrical resistivity ($\text{k}\Omega \text{ cm}$)
Low	> 20
Low to moderate	10–20
High	5–10
Very high	< 5

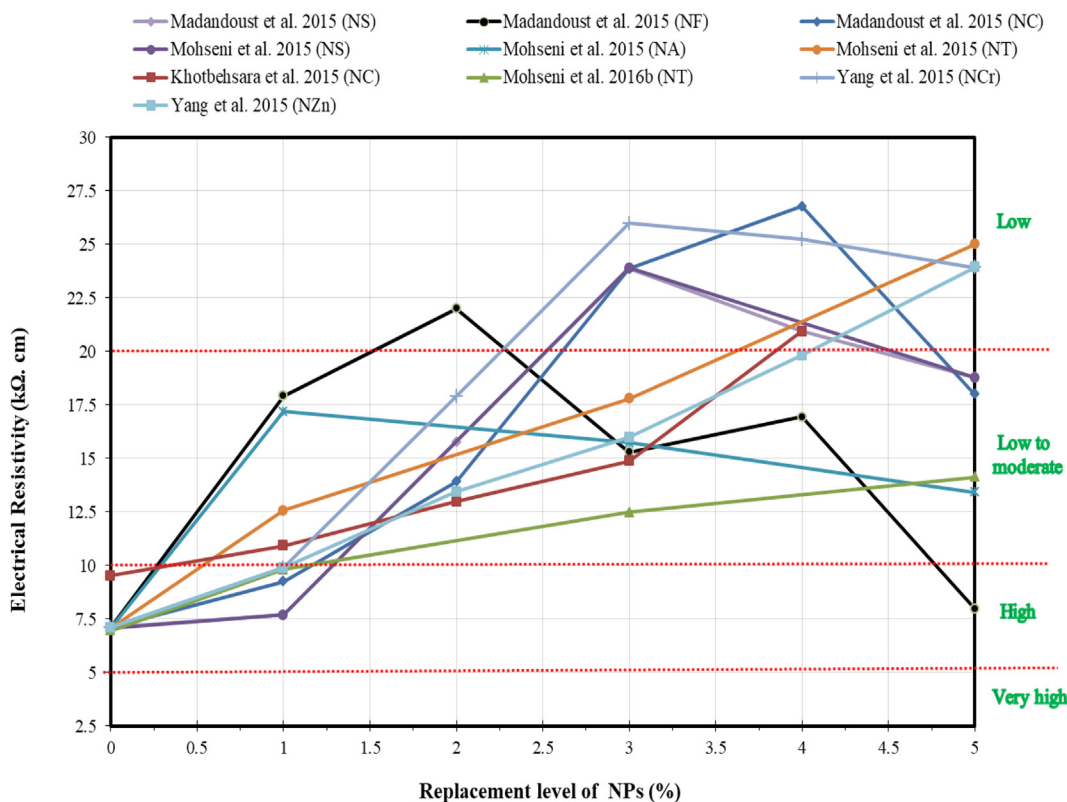


Fig. 9. Electrical resistivity values versus replacement amount of NPs reported in previous studies.

and Tsavdaridis (2016a) found that the optimum percentage of the NA particles regarding the electrical resistivity is 1%, compared to other percentages from 0% to 5%. They observed that the electrical resistivity value increased by about 143% percent when 1% of NA particles were added to the mixture, which shifts the corrosion rate category from high to low-to-moderate.

Moreover, Khotbehsara et al. 2015 reported that the probability of corrosion rate was low for the mixtures made with 4% of NC particles. This can be explained by the fact that the inclusion of NC particles decreases porosity and, therefore, decreases the content of pore water solution in the samples. Predictably, the pore water behaves as an electrolyte for the current, causing a reduction in the pore water solution due to the utilization of NC particles, thus reducing the probability of corrosion. This can be very beneficial for the reinforced concrete structures exposed to chemical and sulfate attacks.

3.3.3. Rapid chloride permeability test (RCPT)

ASTM C1202 standard can be followed to perform the RCPT test. During the test, the amount of charge passed through the specimen is recorded for 6 h by rapid chloride penetration, then the electrical conductance of SCM samples is evaluated. This procedure relies on electrical conductivity, which can be used as an indication to reveal the resistance of the SCMs to chloride ion penetration. ASTM C1202

reported five different performance categories for mixtures according to the charge passed through the specimens as presented in Table 3.

The results extracted from previous studies regarding the impact of NPs on the chloride ion penetration of SCMs are shown in Fig. 10. As shown from the Figure, the addition of NPs changed the chloride permeability category from moderate to low, regardless of NPs type and content. Miyandehi et al. 2014 reported that using NPs has positively impacted the chloride ion penetration of SCMs. They found that SCMs made with 3% of NA particles gave minimum charge passed amongst other combinations and can be located in a category with low chloride permeability. Even though the mixture with 5% NA showed the worst performance compared to other samples, it still belongs to a category with moderate chloride permeability and has more resistance than the control sample (Miyandehi et al. 2014). Moreover, Mohseni et al. 2015 observed that the mixture containing 5% NT provided the minimum charge passed and can be treated with low chloride permeability. Other scholars also presented similar findings (Khotbehsara et al. 2015; Yang et al. 2015). The reduction of chloride ion penetration with the addition of NPs may be attributed to refining the pore structure of the mortar matrix compared to the mixtures without NPs.

4. Modeling the compressive strength of SCMs modified with NPs

As previously mentioned, other mechanical and durability properties can be obtained from compressive strength (CS). Since CS is the most commonly evaluated property among other properties, this section is devoted to predicting the CS of SCMs modified with NPs. In this regard, 292 experimental data from previous papers reported in Table 1 were collected and split into three groups. The first and bigger group comprised 200 datasets utilized to create the models. Each with 46 data points, the second and third groups were utilized to test and validate the models (Faraj et al. 2012b; Ahmed et al. 2021). Since the compressive strength is affected by all mixture ingredients, there-

Table 3
Chloride permeability based on charge passed (ASTM C1202, 2000).

Chloride permeability category	Charge passed (Coulombs)
High	> 4000
moderate	2000–4000
Low	1000–2000
Very low	100–1000
negligible	< 100

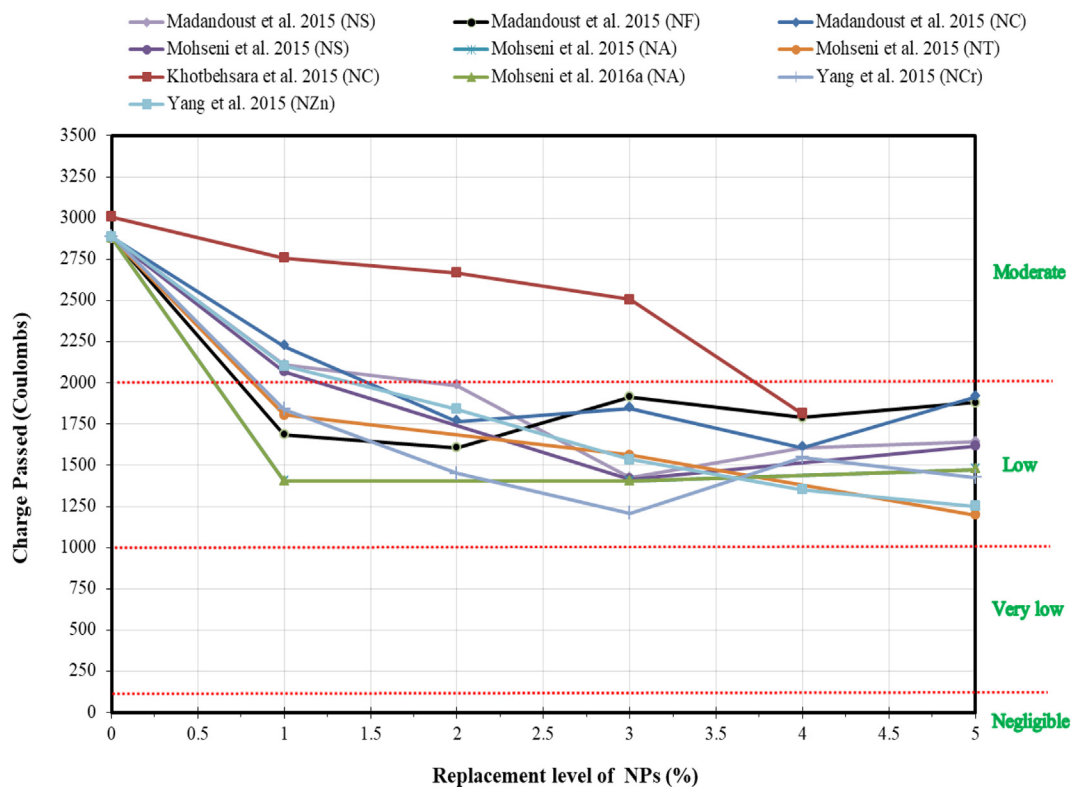


Fig. 10. Charge passed in coulombs versus replacement amount of NPs reported in previous studies.

fore, to develop the models, several independent variables were extracted from previously published papers, including NP% content, cement (C) content in kg/m³, w/b ratio, Superplasticizer (SP) content in kg/m³, fine aggregate (FA) content in kg/m³, and curing time (t) from 3 days to 90 days.

The models developed in this paper are used to estimate the CS of SCMs and choose the best one that offers a better estimate of CS with regard to the CS from measured data. The following assessment criteria were used to compare the predictions of different models: the model had to be scientifically accurate, have a smaller percentage error between observed and measured data, have a lower Mean Absolute Error (MAE), Root Mean Squared Error (RMSE), Objective (OBJ), Scatter Index (SI), and a higher coefficient of determination (R^2) value.

4.1. NLR model

The following Equation (2) may be used to create a nonlinear regression model in general (A. Mohammed et al. 2020; Sarwar et al. 2019). To estimate the CS of typical SCM mixes and SCM mixtures enhanced with NP, the connection between different variables can be expressed in Equation (2) to estimate the CS.

$$\sigma_c = a(C)^c(w/b)^d(t)^e(SP)^f(FA)^g + b(C)^h(w/b)^i(t)^j(SP)^k(FA)^l(NP)^m \quad (2)$$

Where: C stands for the cement content (kg/m³), w/b stands for the water to binder ratio (%), t stands for curing time (days), SP stands for the superplasticizer content (kg/m³), FA stands for fine aggregate (kg/m³), and NP stands for the nanoparticle content (%). Moreover, the model parameters are a, b, c, d, e, f, g, h, i, j, k, l, and calculated based on the least square method.

4.2. MLR model

The MLR, also a regression procedure, can be employed when the predictable variable has a parameter greater than two stages. MLR is

a statistical approach that is comparable to multiple linear regressions. Equation (3) can be used to find the variance between a predictable variable and independent variables.

$$\sigma_c = a(NP)^b(C)^c(w/b)^d(t)^e(SP)^f(FA)^g \quad (3)$$

Equation (3), on the other hand, has a drawback in that it cannot be used to forecast the CS of SCM without NPs content. As a result, the NP content in this model should be larger than zero (NP content > 0%). The least-square approach was used to find the model parameters (a, b, c, d, e, f, and g) as well as model variables.

4.3. ANN model

ANN is a powerful simulation software designed for data analysis and computation to think like a human brain in processing and analyses. This machine learning tool is widely used in construction engineering to predict several numerical problems' future behavior (Sihag et al. 2018; Demircan et al. 2011; Mohammed, 2018). ANN model is generally divided into three main layers: input, hidden, and output layers. Each input and output layer can be one or more layers depending on the proposed problem. However, the hidden layer is usually ranged for two or more layers. Although the input and output layers generally depend on the collected data and the designed model purpose, the hidden layer is determined by rated weight, transfer function, and the bias of each layer to other layers. A multi-layer feed-forward network is built based on a mixture of proportions, weight/bias, and several parameters (NP, Cement, w/b, Curing time, SP, and Fine aggregate) as inputs and output ANN here is the CS. There is no standard approach to designing the network architecture. Therefore, the number of hidden layers and neurons is determined based on a trial and error test. One of the main objectives of the training process of the network is to determine the optimum number of iteration (epochs) that provide the minimum mean absolute error (MAE), and root mean square error (RMSE), and best R^2 -value that is close to

one. The effect of several iterations on reducing the MAE and RMSE has been studied. The collected data set (a total of 292 data) has been divided into three parts for the training purpose of the designed ANN. About 70 percent of the collected data was used as trained data for training the network. The 15 percent of overall data was used to test the data set, and the rest of the remaining data was used to validate the trained network (Faraj et al. 2021b). The designed ANN was trained and tested for various hidden layers to determine optimal network structure based on the fitness of the predicted CS of SCM containing NPs with the CS of the actual collected data. It was observed that the ANN structure with one hidden layer, six neurons, and a hyperbolic tangent transfer function was a best-trained network that provides a maximum R^2 and minimum both MAE and RMSE (shown in Table 4). The general Equation of the ANN model is shown in Equation 4, Equation 5, and 6.

From linear node 0:

$$fc' = \text{Threshold} + \left(\frac{\text{Node1}}{1 + e^{-B1}} \right) + \left(\frac{\text{Node2}}{1 + e^{-B2}} \right) + \dots \quad (4)$$

From sigmoid node 1:

$$B1 = \text{Threshold} + (\text{Attribute} * \text{Variable}) \quad (5)$$

From sigmoid node 2:

$$B2 = \text{Threshold} + (\text{Attribute} * \text{Variable}) \quad (6)$$

5. Assessment criteria for models

Various performance metrics, including the coefficient of determination (R^2), Root Mean Squared Error (RMSE), Mean Absolute Error (MAE), Scatter Index (SI), and OBJ were utilized to analyze and assess the effectiveness of the suggested models, which can be computed using the formulae below:

$$R^2 = \left(\frac{\sum_{p=1}^p (t_p - t') (y_p - y')}{\sqrt{\left[\sum_{p=1}^p (t_p - t')^2 \right] \left[\sum_{p=1}^p (y_p - y')^2 \right]}} \right)^2 \quad (7)$$

$$RMSE = \sqrt{\frac{\sum_{p=1}^p (y_p - t_p)^2}{p}} \quad (8)$$

$$MAE = \frac{\sum_{p=1}^p |(y_p - t_p)|}{p} \quad (9)$$

$$SI = \frac{RMSE}{t'} \quad (10)$$

$$OBJ = \left(\frac{n_{tr}}{n_{all}} * \frac{RMSE_{tr} + MAE_{tr}}{R_{tr}^2 + 1} \right) + \left(\frac{n_{tst}}{n_{all}} * \frac{RMSE_{tst} + MAE_{tst}}{R_{tst}^2 + 1} \right) + \left(\frac{n_{val}}{n_{all}} * \frac{RMSE_{val} + MAE_{val}}{R_{val}^2 + 1} \right) \quad (11)$$

Table 4
The tested ANN architectures.

No. of Hidden layers	No. of Neurons in left side	No. of Neurons in right side	R^2	MAE (MPa)	RMSE (MPa)
1	1	0	0.9126	8.7263	10.6682
1	3	0	0.9873	2.2704	3.001
1	5	0	0.9876	2.3084	3.0413
1	6	0	0.9881	2.3073	3.0369
1	7	0	0.9862	2.631	3.4082
2	1	1	0.9057	9.297	11.3664
2	3	3	0.9866	2.3683	3.1282
2	5	5	0.9871	2.3944	3.1471
2	6	6	0.9874	2.3357	3.0753
2	7	7	0.9864	2.4254	3.2108

Where y_p and t_p are, respectively, the expected and measured values of the path pattern, and t' and y' are the averages of the measured and forecasted values. Training, testing, and validating datasets are referred to as tr, tst, and val, respectively, and n is the number of patterns (collected data) in the associated dataset.

Except for R^2 , the optimum value for all other assessment factors is zero; nevertheless, R^2 has the best value of one. When it comes to the SI parameter, a model has (bad performance) when it is > 0.3 , (fair performance) when it is between 0.2 and 0.3, (good performance) when it is between 0.1 and 0.2, and (great performance) when it is < 0.1 (Li et al. 2013; Golafshani et al. 2020; Ahmed et al., 2022b). In addition, the OBJ parameter was employed as an integrated performance parameter in Equation (11) to measure the efficiency of the suggested models.

6. Results and analysis

6.1. Relationships among forecasted and actual CS

6.1.1. NLR model

Fig. 11a, 11b, and 11c represent the forecasted compressive strength against actual compressive strength obtained from experimental programs of SCM mixes enhanced with NPs for training, testing, and validating datasets, respectively. According to this model, the w/b ratio, cement amount, and SP content are the most critical elements determining SCM mixes' CS. Several experimental programs from previous research confirmed this, reducing the w/b ratio and increasing the amount of cement considerably improving the compressive strength of SCC mixes. The following (Equation (12)) is the proposed Equation for the NLR model with various variable parameters:

$$\sigma_c = 5.63(C)^{3.13}(w/b)^{5.7}(t)^{0.283}(SP)^{-0.40}(FA)^{-1.95} + 0.396(C)^{13.58}(w/b)^{2.608}(t)^{0.046}(SP)^{10.26}(FA)^{-14.78}(NP)^{-0.032} \quad (12)$$

The R^2 , RMSE, and MAE assessment parameters for this model are 0.944, 4.26 MPa, and 3.37 MPa, respectively. Furthermore, the current model's OBJ and SI values for the training dataset are 4.08 and 0.091, respectively.

6.1.2. MLR model

Fig. 12a, 12b, and 12c demonstrate the comparison of estimated CS versus actual CS obtained from experimental programs of SCM mixes enhanced with NPs for training, testing, and validating datasets, respectively. Previous research shows that the most influential parameter that influences the CS of SCM mixes modified with NS is the w/b ratio, similar to the NLR model. The following is the created model for the MLR model with different variable parameters: (Equation (13)):

$$\sigma_c = 8.6 * 10^{-6}(NP)^{-0.052}(C)^{3.307}(w/b)^{1.953}(t)^{0.250}(SP)^{0.653}(FA)^{-0.232} \quad (13)$$

The assessment parameters for this model, such as R^2 , RMSE, and MAE are 0.87, 6.51, MPa and 4.95 MPa, respectively. Moreover, the OBJ and SI values for the current model are 6.05 and 0.136 for the training dataset.

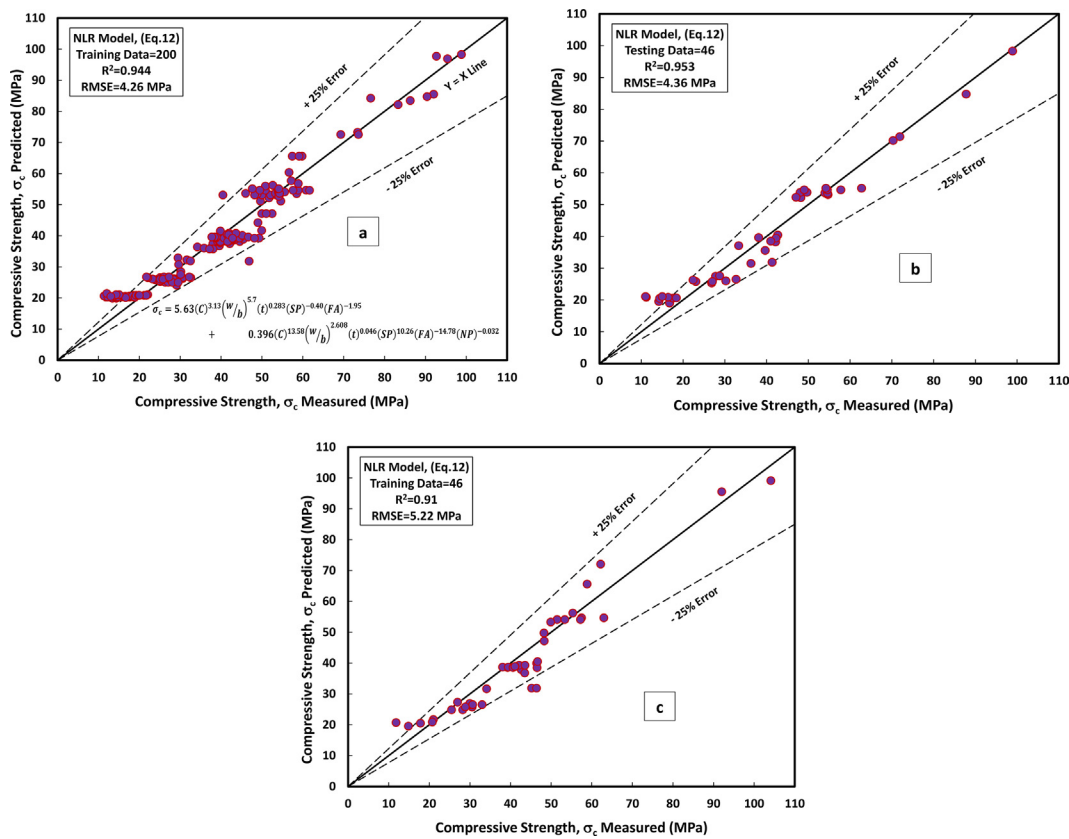


Fig. 11. Comparison between measured and predicted compressive strength of NP modified SCM mixtures using Non-Linear Regression model (NLR) (a) training data, (b) testing data, and (c) validating data.

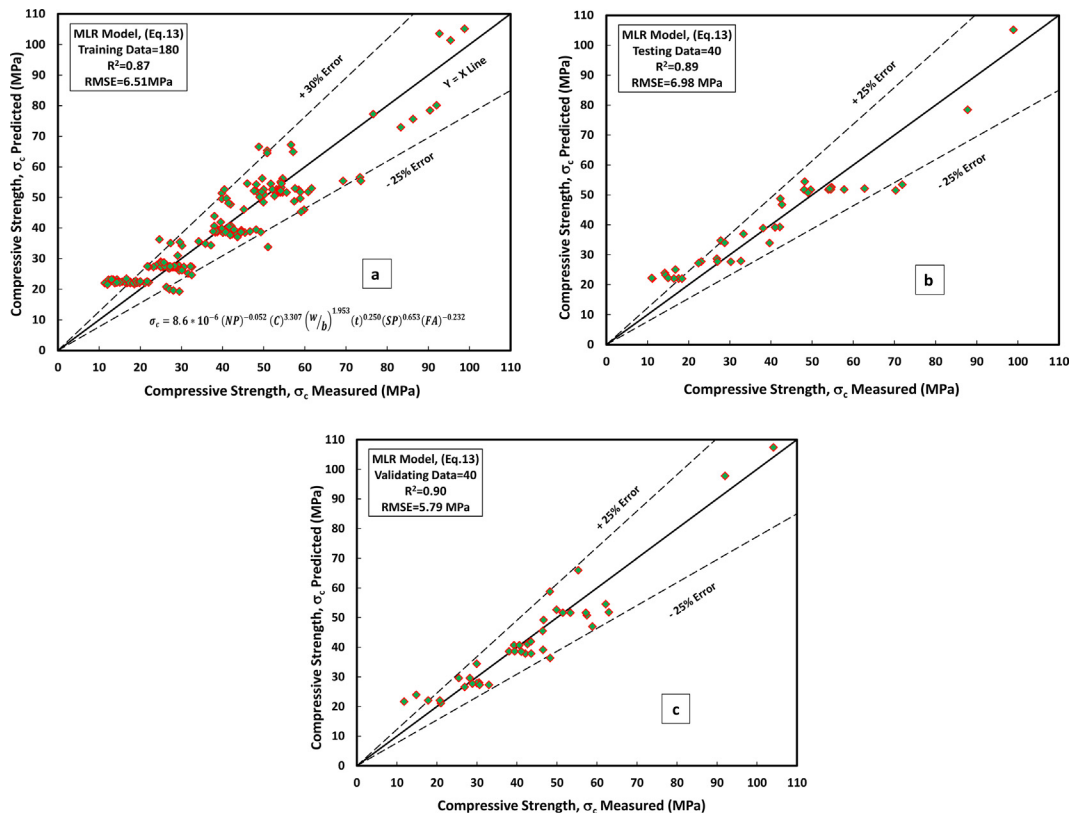


Fig. 12. Comparison between measured and predicted compressive strength of NP modified SCM mixtures using Multi-Linear Regression model (MLR) (a) training data, (b) testing data, and (c) validating data.

6.1.3. ANN model

In this study, the authors tried a lot to get the high efficiency of the ANN by applying different numbers of the hidden layer, neurons, momentum, learning rate, and iteration. Lastly, they observed that when the ANN has one hidden layer, 6 neurons on the left side (as shown in Fig. 13), 0.1 momentum, 0.2 learning rate, and 2000 iteration give best-predicted values of the CS of the SCM. The ANN model was equipped with the training datasets, accompanied by testing and validating datasets to predict the compression strength values for the correct input parameters. The comparison between predicted and measured CS of SCM for training, testing, and validating datasets are presented in Fig. 14a, 14b, and 14c. The studied datasets have a + 20% and -15% error line for the training testing, and validating datasets, which is better than the other developed models. Furthermore, this model has a better performance compared to other models to predict the CS of SCM based on the value of OBJ and SI that illustrated in Fig. 20 and Fig. 21, also, the value of $R^2 = 0.9881$, MAE = 2.3073 MPa, and RMSE = 3.0369 MPa.

6.2. Comparison between developed models

As previously stated, five different statistical methods were used to evaluate the efficacy of the suggested models, including RMSE, MAE, SI, OBJ, and R^2 . In comparison to the NLR and MLR models, the

ANN model has a higher R^2 and lower RMSE and MAE values, as shown in Fig. 15, Fig. 16, and Fig. 17 for R^2 values, RMSE, and MAE, respectively. Fig. 18 also compares model CS estimates for SCM mixtures including NPs based on all data. In addition, Fig. 19 depicts the residual error for all models that use training, testing, and validating datasets. The predicted and measured values of CS for the ANN model are closer in Figs. 18 and 19, indicating that the ANN model outperforms other models.

Fig. 20 shows the OBJ values for all suggested models. The NLR, MLR, and ANN models have 4.08, 6.05, and 3.18, respectively. The OBJ value of the ANN model is 22 percent less than MLR model, and it is also 47.43 percent less than that of the NLR model. This also shows that the ANN model is more efficient when estimating the CS of SCM mixes, including NPs.

Fig. 21 depicts the SI assessment parameter values for the proposed models throughout the training, validating, and testing stages. Fig. 21 shows that the SI values for MLR model for all stages (training, testing, and validating) were between 0.1 and 0.2, suggesting good performance for this model. However, the SI values for the ANN and NLR models were between 0 and 0.1, suggesting that the ANN and NLR models performed excellently. Furthermore, the ANN model, like the other performance factors, has lower SI values when compared to other models. Compared to the MLR model, the ANN model had lower SI values in all stages, for example, 42 percent lower in training and

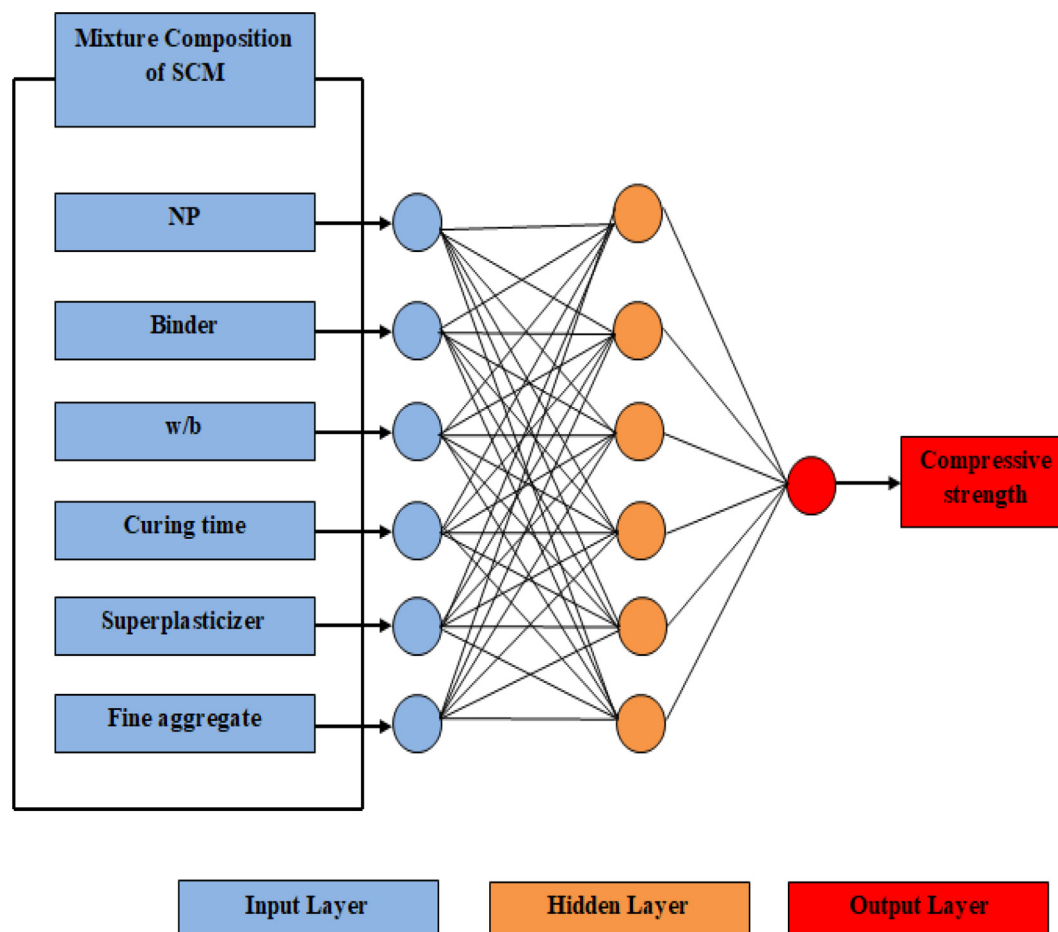


Fig. 13. Optimal Network Structures of the ANN Model.

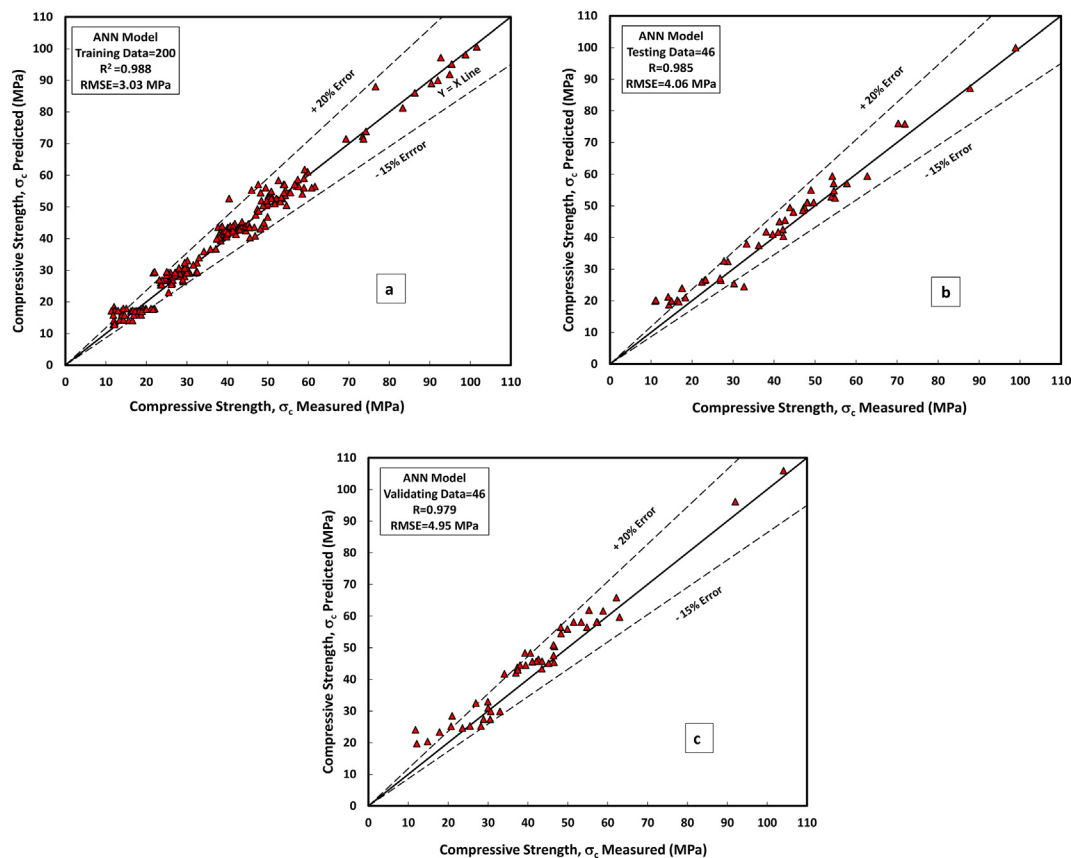


Fig. 14. Comparison between measured and predicted compressive strength of NP modified SCM mixtures using Artificial Neural Network model (ANN) (a) training data, (b) testing data, and (c) validating data.

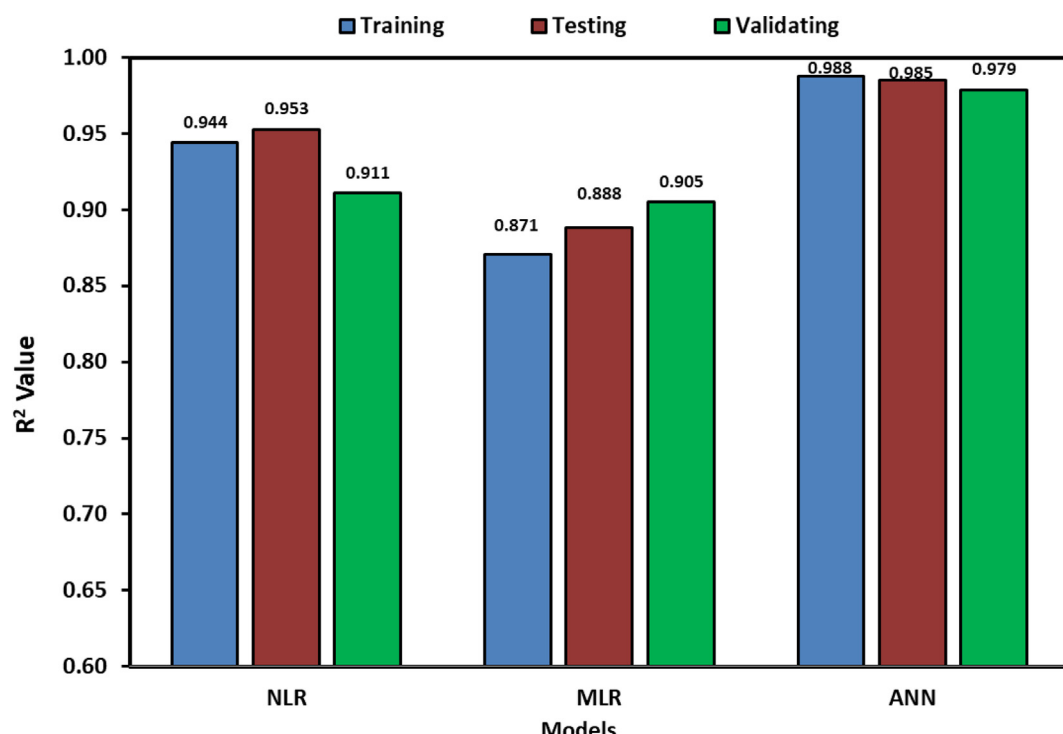


Fig. 15. R^2 values for different proposing models including training, testing, and validating datasets.

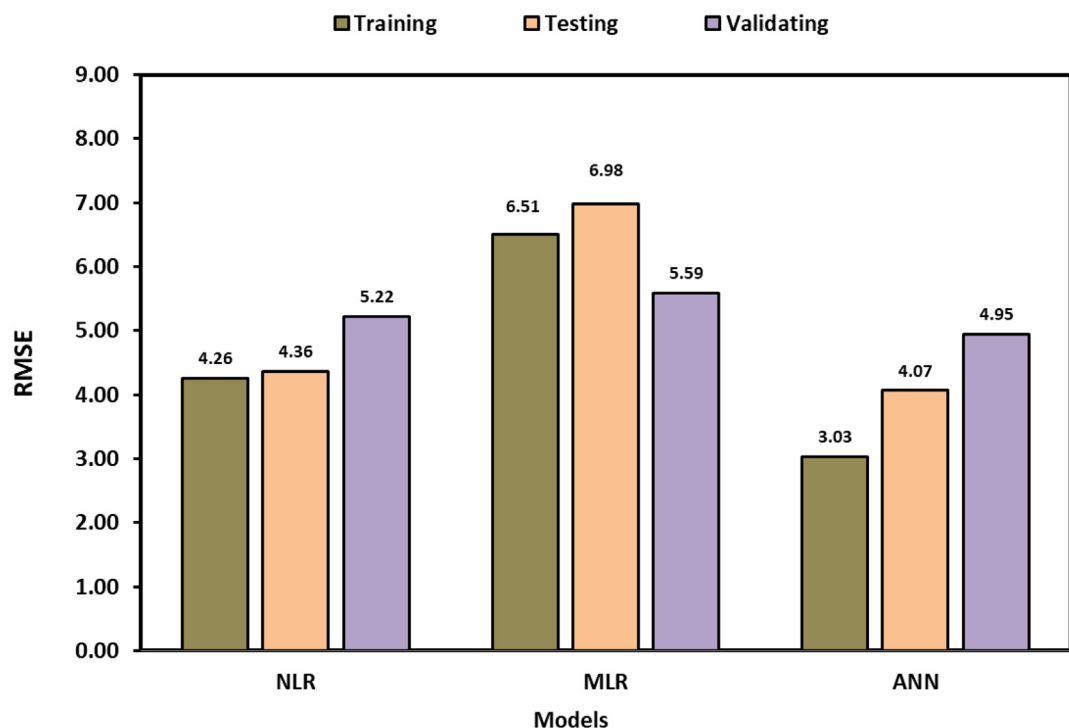


Fig. 16. RMSE values for different proposing models including training, testing, and validating datasets.

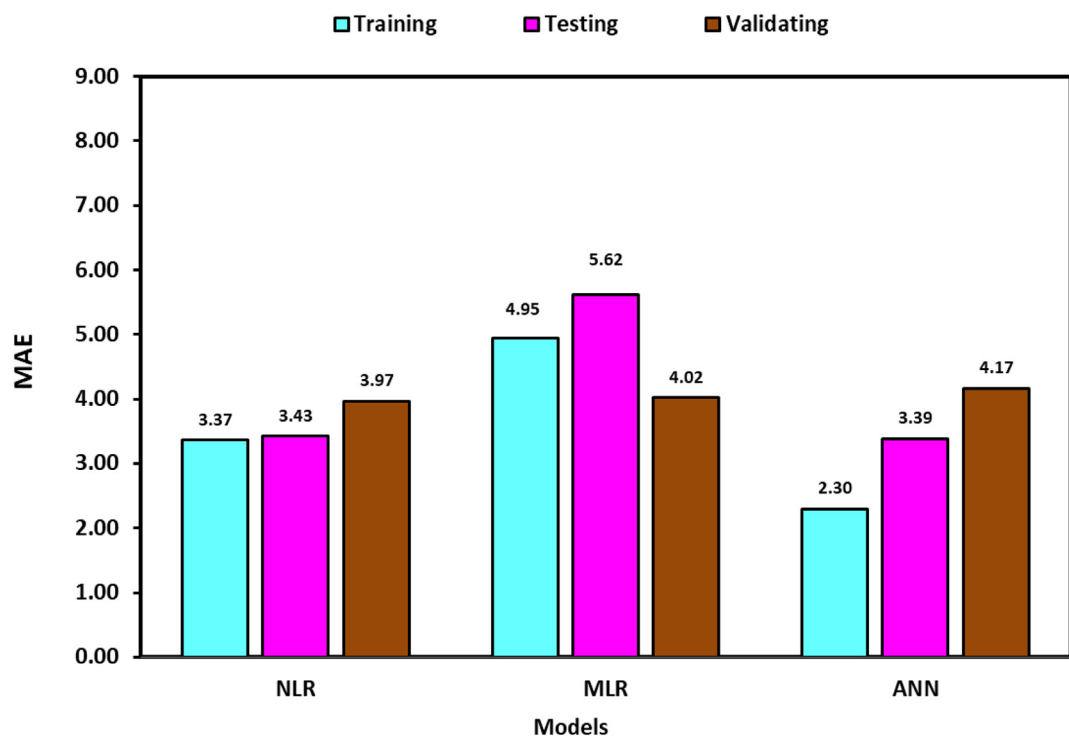


Fig. 17. MAE values for different proposing models including training, testing, and validating datasets.

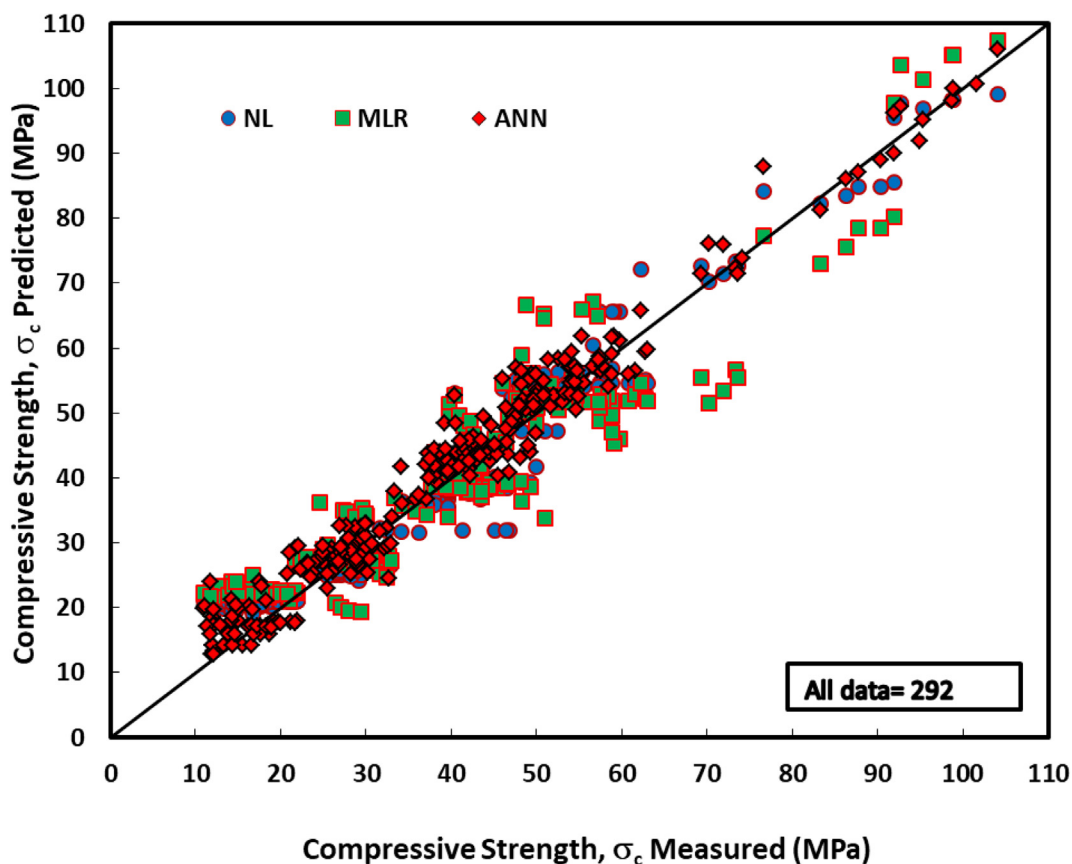


Fig. 18. Comparison between model predictions of compressive strength of SCM mixtures containing NPs using all data.

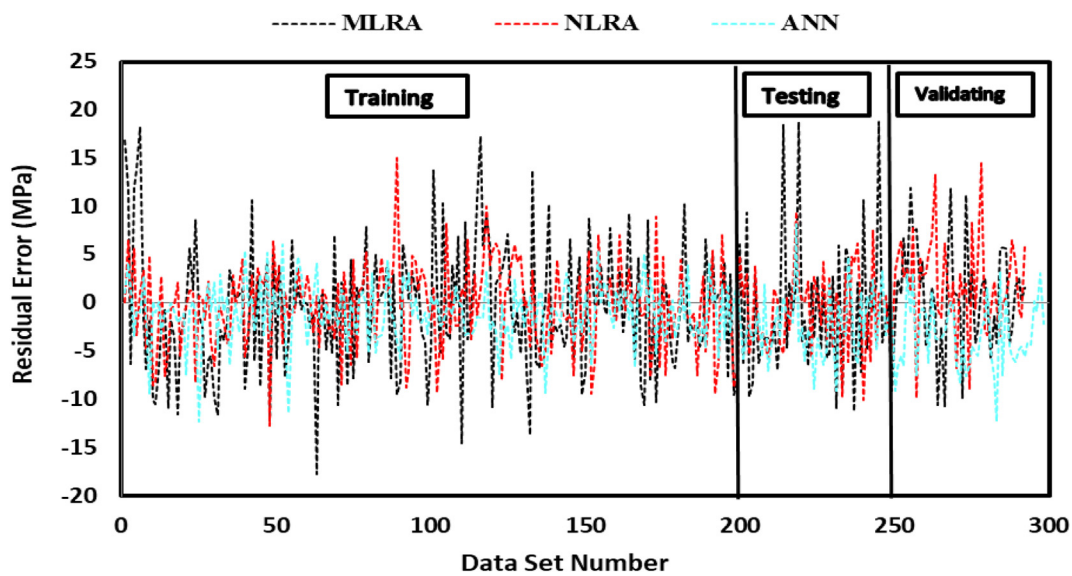


Fig. 19. Variation in predicted values of compressive strength for SCM mixtures containing NPs based on four different approaches in comparison to observed values.

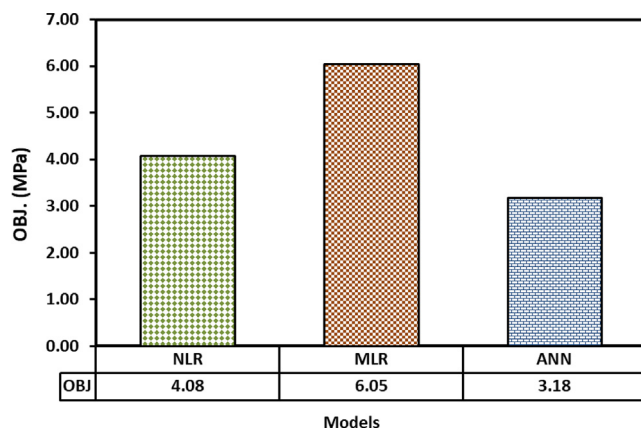


Fig. 20. The OBJ values for all developed models.

26.86 percent lower in testing. This also demonstrated that the ANN model is more efficient and performed better when predicting the CS of SCM mixes, including NPs than the NLR and MLR models.

7. Conclusion

A systematic critical review and modeling were done to highlight the effects of different NPs on the most essential fresh, strength, and durability performance of SCMs. Based on the results available in the literature and the modeling provided in this study, the following conclusions can be drawn:

- Among the different NPs used in the production of SCMs, the NS type is the most common one.

- Different NPs had similar influences on the fresh behavior of SCMs. Generally, increasing the amount of NPs was increased the slump flow diameter and decreased the V-funnel flow time due to higher demand for superplasticizer content.
- Both compressive and flexural strength was slightly increased with increasing NPs content. The optimum percentage for the NPs content was 3% replacement by cement weight, regardless of NPs type. Improving the microstructure due to additional chemical reactions that increase the C-S-H gel is the main factor contributing to improving the strength of SCMs made with NPs.
- The water absorption percentage was considerably decreased due to the addition of NPs. This was related to the fact that the NPs had a very small particle diameter compared to cement particles; thus, during hydration, they fill the small voids between cement particles, resulting in a denser matrix.
- A low probability of corrosion was observed due to the addition of NPs, because with increasing the NP content, the electrical resistivity of SCMs was reduced, which made the composite more corrosion resistant. Regardless of NPs type, the addition of NPs shifted the corrosion rate category from high to low.
- The chloride ion penetration was significantly improved due to the addition of NPs, regardless of their type and content.
- The NLR, MLR, and ANN models were established in this research to predict the CS of SCM mixes. According to the various evaluation criteria, the ANN model outperformed other models with higher R₂ values, lower RMSE, lower MAE, lower OBJ values, and lower SI values for the training, testing, and validating data sets.
- The overall results obtained and reviewed from past studies demonstrated that different types of NPs can efficiently be used to improve the fresh, strength, and durability performance of SCMs; this helps the construction industry further apply nanotechnology for different types of cement-based materials.

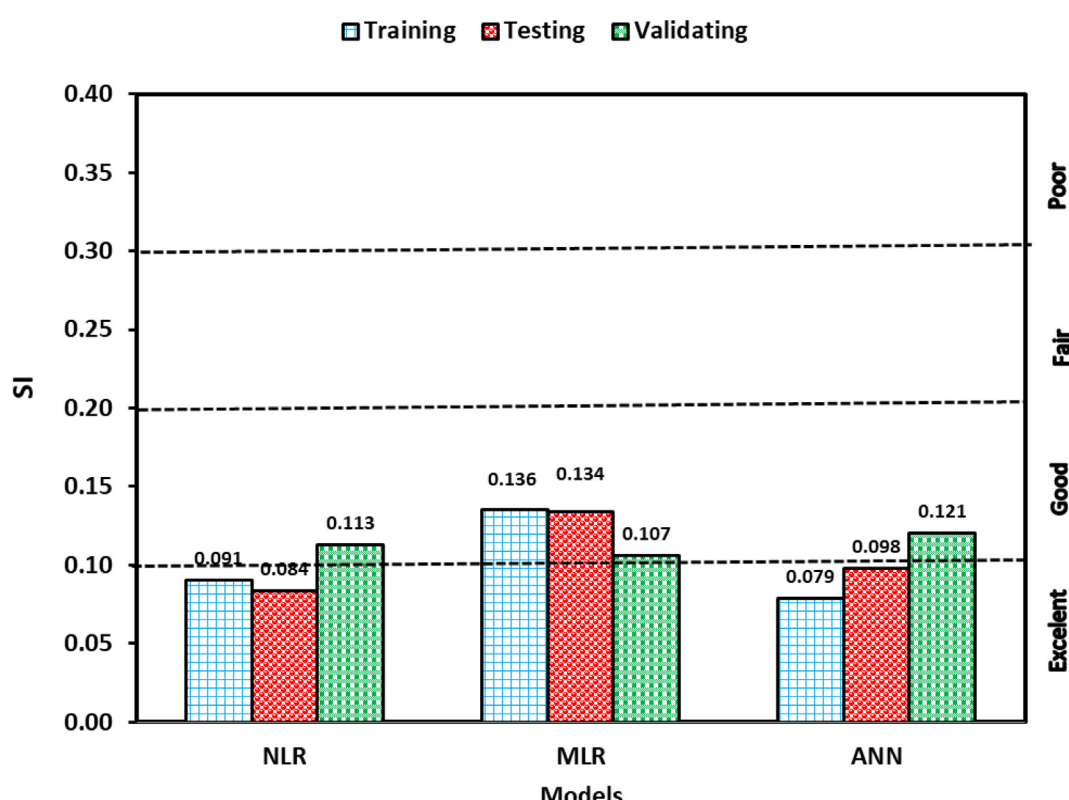


Fig. 21. Comparing the SI performance parameter of different developed models.

Declaration of Competing Interest

The authors declare that they have no known competing financial interests or personal relationships that could have appeared to influence the work reported in this paper.

References

- Ahmed, H.U., Mohammed, A.A., Mohammed, A.S., 2022a. The role of nanomaterials in geopolymer concrete composites: A state-of-the-art review. *Journal of Building Engineering* 49, 104062.
- Ahmed, H. U., Mohammed, A. S., Mohammed, A. A., & Faraj, R. H. (2021). Systematic multiscale models to predict the compressive strength of fly ash-based geopolymer concrete at various mixture proportions and curing regimes. *Plos one*, 16(6), e0253006. <https://doi.org/10.1371/journal.pone.0253006>.
- Ahmed, H.U., Abdalla, A.A., Mohammed, A.S., Mohammed, A.A., Mosavi, A., 2022b. Statistical Methods for Modeling the Compressive Strength of Geopolymer Mortar. *Materials* 15, 1868. <https://doi.org/10.3390/ma15051868>.
- Balapour, M., Joshaghani, A., Althoei, F., 2018. Nano-SiO₂ contribution to mechanical, durability, fresh and microstructural characteristics of concrete: A review. *Construction and Building Materials* 181, 27–41. <https://doi.org/10.1016/j.conbuildmat.2018.05.266>.
- Demircan, E., Harendra, S., Vipulanandan, C., 2011. Artificial neural network and nonlinear models for gelling time and maximum curing temperature rise in polymer grouts. *Journal of materials in civil engineering* 23 (4), 372–377. [https://doi.org/10.1061/\(ASCE\)MT.1943-5533.0000172](https://doi.org/10.1061/(ASCE)MT.1943-5533.0000172).
- Efnarc, 2002. *Specifications and guidelines for self-consolidating concrete*. Surrey, UK: European Federation of Suppliers of Specialist Construction Chemicals (Efnarc).
- Faraj, R.H., Hama Ali, H.F., Sherwani, A.F.H., Hassan, B.R., Karim, H., 2020. Use of recycled plastic in self-compacting concrete: A comprehensive review on fresh and mechanical properties. *Journal of Building Engineering* 30, 101283.
- Faraj, R.H., Mohammed, A.A., Omer, K.M., 2022. Self-compacting concrete composites modified with nanoparticles: A comprehensive review, analysis and modeling. *Journal of Building Engineering* 50, 104170.
- Faraj, R.H., Mohammed, A.A., Mohammed, A., Omer, K.M., Ahmed, H.U., 2021a. Systematic multiscale models to predict the compressive strength of self-compacting concretes modified with nanosilica at different curing ages. *Engineering with Computers* 1–24. <https://doi.org/10.1007/s00366-021-01385-9>.
- Faraj, R.H., Sherwani, A.F.H., Daraei, A., 2019. Mechanical, fracture and durability properties of self-compacting high strength concrete containing recycled polypropylene plastic particles. *Journal of Building Engineering* 25, <https://doi.org/10.1016/j.jobe.2019.100808> 100808.
- Faraj, R.H., Sherwani, A.F.H., Jafer, L.H., Ibrahim, D.F., 2021b. Rheological behavior and fresh properties of self-compacting high strength concrete containing recycled PP particles with fly ash and silica fume blended. *Journal of Building Engineering* 34, 101667.
- Golafshani, E.M., Behnood, A., Arashpour, M., 2020. Predicting the compressive strength of normal and High-Performance Concretes using ANN and ANFIS hybridized with Grey Wolf Optimizer. *Construction and Building Materials* 232, <https://doi.org/10.1016/j.conbuildmat.2019.117266> 117266.
- Jalal, M., Teimortashlu, E., Grasley, Z., 2019. Performance-based design and optimization of rheological and strength properties of self-compacting cement composite incorporating micro/nano admixtures. *Composites Part B: Engineering* 163, 497–510. <https://doi.org/10.1016/j.compositesb.2019.01.028>.
- Kadhim, A.S., Atiyah, A.A., Salih, S.A., 2020. Properties of self-compacting mortar containing nano cement kiln dust. *Materials Today: Proceedings* 20, 499–504. <https://doi.org/10.1016/j.matpr.2019.09.177>.
- Khotbehsara, M.M., Miyandehi, B.M., Naseri, F., Ozbaakkaloglu, T., Jafari, F., Mohseni, E., 2018. Effect of SnO₂, ZrO₂, and CaCO₃ nanoparticles on water transport and durability properties of self-compacting mortar containing fly ash: Experimental observations and ANFIS predictions. *Construction and Building Materials* 158, 823–834. <https://doi.org/10.1016/j.conbuildmat.2017.10.067>.
- Khotbehsara, M.M., Mohseni, E., Yazdi, M.A., Sarker, P., Ranjbar, M.M., 2015. Effect of nano-CuO and fly ash on the properties of self-compacting mortar. *Construction and Building Materials* 94, 758–766. <https://doi.org/10.1016/j.conbuildmat.2015.07.063>.
- Courard, L., Darmont, A., Willem, X., Geers, C., Degeimbre, R., 2002. Repairing concretes with self-compacting concrete: testing methodology assessment, in: In: Proceeding of the 1st North American Conference on the Design and Use of Self-consolidating Concrete, pp. 267–274.
- Lazaro, A., Yu, Q.L., Brouwers, H.J.H., 2016. Nanotechnologies for sustainable construction. In: Sustainability of construction materials. Woodhead Publishing, pp. 55–78.
- Li, M.F., Tang, X.P., Wu, W., Liu, H.B., 2013. General models for estimating daily global solar radiation for different solar radiation zones in mainland China. *Energy conversion and management* 70, 139–148. <https://doi.org/10.1016/j.enconman.2013.03.004>.
- Madandoust, R., Mohseni, E., Mousavi, S.Y., Namnevis, M., 2015. An experimental investigation on the durability of self-compacting mortar containing nano-SiO₂, nano-Fe₂O₃ and nano-CuO. *Construction and Building Materials* 86, 44–50. <https://doi.org/10.1016/j.conbuildmat.2015.03.100>.
- Miyandehi, B.M., Behforouz, B., Khotbehsara, E.M., Balgouri, H.A., Fathi, S., Khotbehsara, M.M., 2014. An experimental investigation on nano-Al₂O₃ based self-compacting mortar. *J. Am. Sci* 10 (11), 229–233.
- Mohammed, A.S., 2018. Vipulanandan models to predict the electrical resistivity, rheological properties and compressive stress-strain behavior of oil well cement modified with silica nanoparticles. *Egyptian journal of petroleum* 27 (4), 1265–1273. <https://doi.org/10.1016/j.ejpe.2018.07.001>.
- Mohammed, A., Mahmood, W., Ghafor, K., 2020. TGA, rheological properties with maximum shear stress and compressive strength of cement-based grout modified with polycarboxylate polymers. *Construction and Building Materials* 235, <https://doi.org/10.1016/j.conbuildmat.2019.117534>.
- Mohseni, E., Miyandehi, B.M., Yang, J., Yazdi, M.A., 2015. Single and combined effects of nano-SiO₂, nano-Al₂O₃ and nano-TiO₂ on the mechanical, rheological and durability properties of self-compacting mortar containing fly ash. *Construction and Building Materials* 84, 331–340.
- Mohseni, E., Naseri, F., Amjadi, R., Khotbehsara, M.M., Ranjbar, M.M., 2016b. Microstructure and durability properties of cement mortars containing nano-TiO₂ and rice husk ash. *Construction and Building Materials* 114, 656–664. <https://doi.org/10.1016/j.conbuildmat.2016.03.136>.
- Mohseni, E., Tsavdaridis, K.D., 2016a. Effect of nano-alumina on pore structure and durability of Class F Fly ash self-compacting mortar. *American Journal of Engineering and Applied Sciences* 9 (2), 323–333. <https://doi.org/10.3844/ajeassp.2016.323.333>.
- Nasr, D., Behforouz, B., Borujeni, P.R., Borujeni, S.A., Zehtab, B., 2019. Effect of nano-silica on mechanical properties and durability of self-compacting mortar containing natural zeolite: Experimental investigations and artificial neural network modeling. *Construction and Building Materials* 229, <https://doi.org/10.1016/j.conbuildmat.2019.116888> 116888.
- Rao, S., Silva, P., De Brito, J., 2015. Experimental study of the mechanical properties and durability of self-compacting mortars with nano materials (SiO₂ and TiO₂). *Construction and Building Materials* 96, 508–517. <https://doi.org/10.1016/j.conbuildmat.2015.08.049>.
- Sarwar, W., Ghafor, K., Mohammed, A., 2019. Modeling the rheological properties with shear stress limit and compressive strength of ordinary Portland cement modified with polymers. *Journal of Building Pathology and Rehabilitation* 4 (1), 1–12. <https://doi.org/10.1007/s41024-019-0064-6>.
- Shahbazpanahi, S., Faraj, R.H., 2020. Feasibility study on the use of shell sunflower ash and shell pumpkin ash as supplementary cementitious materials in concrete. *Journal of Building Engineering* 30, <https://doi.org/10.1016/j.jobe.2020.101271> 101271.
- Shahbazpanahi, S., Manie, S., Faraj, R.H., Seraji, M., 2021a. Feasibility study on the use of tagouk ash as pozzolanic material in concrete. *Clean Technologies and Environmental Policy* 23 (4), 1283–1294. <https://doi.org/10.1007/s10098-020-0211-8>.
- Shahbazpanahi, S., Tajara, M.K., Faraj, R.H., Mosavi, A., 2021b. Studying the C-H crystals and mechanical properties of sustainable concrete containing recycled coarse aggregate with used nano-silica. *Crystals* 11 (2), 122. <https://doi.org/10.3390/crust11020122>.
- Sharif, H.H., 2021. Fresh and Mechanical Characteristics of Eco-efficient Geopolymer Concrete Incorporating Nano-silica: An Overview. *Kurdistan Journal of Applied Research*, 64–74 <https://doi.org/10.24017/science.2021.2.6>.
- Sihag, P., Jain, P., Kumar, M., 2018. Modelling of impact of water quality on recharging rate of storm water filter system using various kernel function based regression. *Modeling earth systems and environment* 4 (1), 61–68. <https://doi.org/10.1007/s40808-017-0410-0>.
- Thomas, B.S., Kumar, S., Arel, H.S., 2017. Sustainable concrete containing palm oil fuel ash as a supplementary cementitious material—A review. *Renewable and Sustainable Energy Reviews* 80, 550–561. <https://doi.org/10.1016/j.rser.2017.05.128>.
- Yang, J., Mohseni, E., Behforouz, B., Khotbehsara, M.M., 2015. An experimental investigation into the effects of Cr₂O₃ and ZnO₂ nanoparticles on the mechanical properties and durability of self-compacting mortar. *International Journal of Materials Research* 106 (8), 886–892. <https://doi.org/10.3139/146.111245>.
- Zhu, W., Bartos, P. J., & Porro, A. (2004). Application of nanotechnology in construction. *Materials and structures*, 37(9), 649–658. <https://doi.org/10.1007/BF02483294>.